

Simulation of the Performance of IEEE 802.16-2004 Fixed Broadband Wireless Access Technology

by

Saideepthi Katragunta

Problem report submitted to the
College of Engineering and Mineral Resources
at West Virginia University
in partial fulfillment of the requirements
for the degree of

Master of Science
in
Electrical Engineering

Matthew C.Valenti, Ph.D., Chair
Brian D.Woerner, Ph.D., Co-Chair
Natalia A.Schmid, Ph.D.

Lane Department of Computer Science and Electrical Engineering

Morgantown, West Virginia
2007

Keywords: Broadband wireless access, MIMO, space time codes, turbo codes

Copyright 2007 Saideepthi Katragunta

Abstract

Simulation of the Performance of IEEE 802.16-2004 Fixed Broadband Wireless Access
Technology

by

Saideepthi Katragunta
Master of Science in Electrical Engineering

West Virginia University

Matthew C.Valenti, Ph.D., Chair

The explosive growth of the Internet over the last decade has led to an increasing demand for high-speed, ubiquitous Internet access. Fixed broadband wireless access (BWA) is an ideal solution for providing high data rate communications, where traditional wireline technologies like digital subscriber line (DSL) and cable modems are either unavailable or too costly to be installed. IEEE 802.16-2004, also known as WiMax, is a standard that promotes the deployment of fixed broadband wireless access. To achieve this, the IEEE 802.16-2004 standard specifies three air interfaces which include WirelessMAN-SCa, WirelessMAN-OFDM, and WirelessMAN-OFDMA to operate in a non-line-of-sight (NLOS) environment within the licensed frequencies below 11 GHz.

In this project, we simulate the performance of the WirelessMAN-SCa option of the IEEE 802.16-2004 standard. First we provide an overview of the physical layer features and the channel model of a WiMax system. We show the advantages of using multiple-input-multiple-output (MIMO) techniques to combat the fading effects in a wireless channel. The design of a convolutional turbo code (CTC), used as an optional error correction technique by IEEE 802.16-2004 is described. For the Alamouti space time block code (STBC), considering the two transmit and one receive antenna case, we derive the equations for the log likelihood ratios (LLRs) to be given as inputs to the CTC decoder. STBC gives diversity gain, CTC gives coding gain, and a concatenation of both STBC and CTC simultaneously achieves diversity and coding gain.

Acknowledgments

I am very grateful to Dr. Brian Woerner for giving me an opportunity to do research and for suggesting me this excellent topic to work on. I can undoubtedly say he is one of the best persons I have known. My sincere thanks to Dr. Matthew Valenti for agreeing to be my advisor and guiding me through the entire sequence of my Problem report. I admire his work and talent. His suggestions were of such great help. I thank Dr. Natalia Schmid for being my committee member and supporting me.

I would like to thank all my friends for making my life at WVU so easy and memorable. Finally, I would like to thank my dad K. Rajendra Prasad, mom K.Vijaya Lakshmi and my brother K. Hari Krishna. Whatever I achieve in my life is due to their love and support.

Contents

Acknowledgments	iii
List of Figures	vi
1 Introduction to Broadband Technology	1
1.1 Report Outline	3
2 WiMax System Overview	5
2.1 Standards for Fixed Broadband Wireless Access	5
2.1.1 Frequency Band 10-66 GHz	5
2.1.2 Frequency Bands 11 GHz and Below	6
2.2 WirelessMAN-SCa Physical Layer	7
2.3 Digital Modulation Schemes	8
2.3.1 Representation of Communication Signals	8
2.3.2 M-ary Phase Shift Keying (MPSK)	9
2.3.3 Constellation Mapping	10
2.4 Wireless Channel	11
2.4.1 Rayleigh Fading Distribution	12
2.4.2 Block Fading	13
2.4.3 Performance of BPSK and QPSK	13
2.5 Summary	14
3 Multiple Antenna Systems	16
3.1 Introduction to Diversity	16
3.1.1 Diversity Combining Techniques	17
3.2 MIMO Techniques	21
3.2.1 Space-Time Block Codes	22
3.2.2 Space-Time Trellis Coding	27
3.2.3 BLAST Techniques	27
3.3 Summary	30
4 Turbo Coding for WiMax	31
4.1 Channel Coding for WiMax-IEEE 802.16-2004	31
4.2 The need for Channel Coding	31
4.3 Convolutional Turbo Coder	33

4.3.1	Introduction	33
4.3.2	CTC Encoder	33
4.3.3	CTC Interleaver	35
4.3.4	CTC Puncturer	36
4.4	CTC Decoder	37
4.4.1	Calculation of the input LLRs to the decoder	37
4.5	Summary	40
5	Results and Conclusions	41
5.1	Performance of Concatenated STBC and CTC for WiMax	41
5.1.1	System Model for BWA Applications	41
5.2	Results	43
5.3	Conclusions	43
5.4	Future Work	44
	References	47

List of Figures

2.1	WirelessMAN-SCa PHY simulator.	7
2.2	Constellation mapping for BPSK and QPSK with Gray encoding.	11
2.3	SNR vs BER for BPSK in AWGN and fading.	15
3.1	Diversity Combining at the Receiver.	18
3.2	Bit error rate of BPSK (lower curve) and QPSK (higher curve) in a fading channel for $L = 1, 2, 3$ with MRC decoding	20
3.3	Alamouti space time block code with QPSK in Rayleigh fading channel with MRC decoding.	25
3.4	V-BLAST	28
3.5	V-BLAST for QPSK using ML detector	30
4.1	CTC encoder with a Constituent encoder.	34
4.2	Circulation State Look up Table for IEEE 802.16-2004.	36
5.1	Concatenated STBC and CTC BER curves for code rates $1/3, 1/2,$ and $3/4$	44
5.2	Throughput curves for concatenated STBC and CTC for rates $1/3, 1/2$ and $3/4$	44
5.3	Comparison of coded and uncoded STBC for rate $1/3$	45
5.4	Comparison of SISO-CTC, uncoded STBC and coded STBC	45

Chapter 1

Introduction to Broadband Technology

Internet services and applications continue to evolve and expand. Presently, there are also consumers who access the Internet over relatively low-speed dial-up connections which involves additional delays and inconvenience resulting from the need to establish a connection each time an Internet session is established. For the Internet to realize its true potential as a platform for global communications infrastructure supporting integrated, interactive multimedia services, consumers will need “always on” broadband access. There is no single definition of what constitutes broadband Internet access. In general, a broadband connection allows users to download web pages and files more quickly and facilitates new applications such as streaming audio/video and interactive services such as video conferencing and Internet telephony. More technically, broadband is a transmission facility having the bandwidth to carry multiple data, voice, and video channels all at once [1]. As of today, broadband access is provided by a series of technologies like telephony (DSL), cable (cable modems), satellite, fixed/mobile wireless access. Although they use different transmission methods and technologies, they all provide consumers with the same service: high-speed communications and data connectivity. While digital subscriber line (DSL) and cable modems are the most extensively deployed broadband technologies to date, broadband wireless access (BWA) is still an emerging technology with many advantages over wired access. Both DSL and cable modems require the modification of an existing physical infrastructure i.e. telephone lines

and cable television respectively.

Digital Subscriber Line (DSL) DSL technology makes use of the capacity of conventional telephone lines to transmit data at a higher frequency along with the low frequency voice signals. Data transmission rate of an asynchronous digital subscriber line (ADSL) ranges from 7 Mbps for downloading to 1 Mbps for uploading. The access speed remains constant even during peak usage hours as each user is allocated a separate bandwidth. The major disadvantage of ADSL is that it is distance sensitive, i.e. the performance depends on how far the user is from the telephone company's central office and also sometimes its range might be out of reach for many customers (should be within 3 miles) [2].

Cable Modems With some modifications, cable TV networks have the ability to provide broadband access through cable modems. For this the users have to be within the range of the broadband capable cable infrastructure. Download speeds ranging from 3-10 Mbps and upload speeds from 128 Kbps to 10 Mbps are possible using this technology. As the cable network is shared by several users, unlike in DSL technology, the access speed might reduce during the peak usage hours. One more disadvantage of cable modem technology is its broadcast nature which leads to security concerns [2].

In spite of the existence of technologies like DSL and cable modems, the access of broadband by most people, especially people living in rural and remote areas, is very limited and also the costs of laying new telephone lines and cables to these inaccessible locations is very high. Due to all the above disadvantages of wired access, the growth of alternate wireless broadband technology is expanding. Wireless broadband techniques provide better performance compared to DSL and cable with lower cost, ease of installation and be available to any geographic location.

The IEEE 802.16 standards body, also known as WiMax, specifies standards to promote the access of wireless broadband. The WiMax setup is similar to that of a cellular system setup where base stations are used to serve a radius of several miles [3]. But WiMax operates in much higher frequency bands like 10-66 GHz for line of sight (LOS) operation and 2-11 GHz for non line of sight operation (NLOS). The two key issues involved in the design of a wireless system are fading and interference over the channel. Therefore the physical and MAC layers of such systems should include several advanced features like orthogonal frequency division

multiplexing (OFDM), multiple-input-multiple-output (MIMO), adaptive modulation and coding, automatic repeat request (ARQ) in order to mitigate the impairments (fading and interference) of the NLOS environment to achieve high-data-rates and high-quality. This project focusses on the improvement of the performance of fixed broadband wireless access systems by introducing multiple antennas (MIMO) at the transmitting and receiving ends of the wireless link in combination with signal processing and forward error correction (FEC) coding. The use of multiple antennas both at the base station (BS) and/or at the subscriber station (SS) improves the coverage area, link reliability and data rate of the wireless system [4]. The turbo code that we used for error control coding provides very low bit error rates compared to other existing channel codes with no additional power requirement which made their way into the 3G wireless systems, digital video broadcast (DVB) systems, and emerging WiFi, WiMax systems.

1.1 Report Outline

The IEEE 802.16-2004 standard [5] consolidated the previous IEEE 802.16 standards to provide fixed broadband wireless access by specifying three air interfaces to operate in the licensed frequencies below 11 GHz (NLOS operation). They are WirelessMAN-SCa, WirelessMAN-OFDM, WirelessMAN-OFDMA. This project simulates the performance of WirelessMAN-SCa which is for a single carrier.

In Chapter 2, first the physical layer features of the WirelessMAN-SCa system are described and in general the representation of the wireless signals and wireless channel is studied. The fading characteristics of the wireless channel and the different forms of fading that a wireless signal can experience are discussed. The wireless channel model, the modulation techniques and the performance criteria (BER) that we consider for our simulations are studied. The emphasis of this project will be on Chapter 3 where MIMO is introduced to provide spatial diversity in the wireless channel. The two major MIMO techniques, space time block codes (STBC) and spatial multiplexing (SM), are discussed and their performance curves are shown. As we use the Alamouti STBC algorithm in our WiMax implementation, the maximal ratio receiver combining (MRRC) scheme used at the receiver to decode the STBC

is discussed in detail. Chapter 4 is about the channel coding schemes that are specified by the standards. We focus on the convolutional turbo coding (CTC) scheme and will describe its encoder structure which uses a duobinary circular recursive systematic convolutional code (CRSC). The soft inputs, i.e. the log likelihood ratios (LLRs) that should be given to the turbo decoder input, are derived considering a two transmit one receive STBC with MRC decoding. In the final chapter, the STBC - CTC concatenated results, i.e. the BER curves obtained by concatenating the Alamouti space time block code and the convolutional turbo code, are shown.

Chapter 2

WiMax System Overview

2.1 Standards for Fixed Broadband Wireless Access

As there is an increasing demand for high data rate communications to transmit data, voice, and video at feasible cost and complexity, wireless broadband access provides a good solution. The IEEE 802.16 standard, often referred to as WiMax, aims to provide wireless broadband services on the scale of a metropolitan area network (MAN). WiMax is designed to operate in frequency bands 10-66 GHz for LOS propagation and below 11 GHz for NLOS propagation [5]. The previous fixed broadband wireless access (BWA) standards like IEEE 802.16, IEEE 802.16a, IEEE 802.16c which only operated in their individual frequency bands have been consolidated to a single standard IEEE 802.16-2004 (WiMax) to support multiple services. It specifies air interface which includes the design of the medium access (MAC) layer and the multiple physical (PHY) layer specifications [5]. In this chapter we give a brief description of the MAC layer and focus on the physical layer design in detail. The goal of this project is to use computer simulation to produce performance results of the WiMax system which are included in Chapter 5. These results are obtained by simulating various physical layer features given in the IEEE 802.16-2004 standard [5].

2.1.1 Frequency Band 10-66 GHz

The 10-66 GHz band was the first licensed frequency band used to standardize BWA. Due to the higher frequencies and hence the shorter wavelengths in this band, the electromagnetic

waves get attenuated severely by different terrain and due to the high path loss. The physical environment is such that there cannot be any significant multipath and hence line of sight (LOS) is a requirement. In the 10-66 GHz frequency band, WiMax is designed to achieve data rates up to 120 Mbps and such physical environment is well suited for point-to-multipoint (PMP) access which include at least one base station (BS) and several subscriber stations (SS). The WiMax system with the above PHY specifications serves from small office/home office (SOHO) through medium to large office applications. The single carrier modulation air interface specified for this 10-66 GHz frequency band is known as “WirelessMAN-SC” air interface [5] .

2.1.2 Frequency Bands 11 GHz and Below

In order to provide broadband wireless access for the residential areas where LOS propagation is not feasible, the licensed frequency bands of 11 GHz and below are to be considered. At these frequencies due to the longer wavelengths, there is no need for LOS and also multipath propagation may be significant. Therefore, in order that this system has to support both LOS and NLOS propagation, the PHY has to be robust with more advanced features like multiple antennas, power management techniques and interference mitigation techniques. Additional MAC features such as automatic repeat request (ARQ) for retransmission of data, and mesh topology in addition to PMP are supported [5]. In a mesh mode, subscriber stations can communicate directly with one another. In this case, a station that does not have LOS with the base station can get its traffic from another station [6].

The PHY design at these frequencies is challenging because of the interference. Hence, the standard supports burst-by-burst adaptivity for the modulation and coding schemes and specifies three interfaces [6]. They are **WirelessMAN-SCa** which uses single carrier modulation, **WirelessMAN-OFDM** which uses 256-carrier orthogonal frequency division multiplexing and provides multiple access to different stations through time-division multiple access, and **WirelessMAN-OFDMA** which uses a 2048 carrier OFDM scheme by providing orthogonal frequency division multiple access to different stations. For the license-exempt bands below 11 GHz, though the physical environment is the same as licensed bands,

there are additional interference and co-existence issues [7]. To overcome these, a feature known as dynamic frequency selection (DFS) is introduced by the MAC layer to detect and avoid interference. The DFS scheme chooses the frequency that allows high performance, and this scheme differentiates between primary user interference and cochannel interference [6]. Implementation of WiMax exclusively for the license-exempt bands comply with **WirelessHUMAN** standard along with the standards mentioned above [5]. In this report, we focus on the WirelessMAN-SCa standard for licensed frequency band by describing its physical layer further in detail and simulating the performance of this PHY standard.

2.2 WirelessMAN-SCa Physical Layer

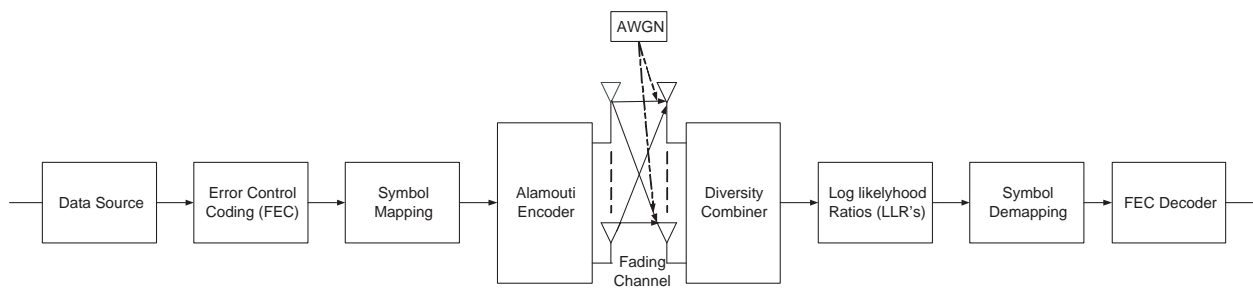


Figure 2.1: WirelessMAN-SCa PHY simulator.

Fig. 2.1 shows the block diagram representation of the physical layer, which is implemented in this project. Designing a communication system for a wireless channel is much more challenging than for a wired channel because of its random varying nature. As it includes multipath fading distortion in addition to additive white Gaussian noise (AWGN), features like error control coding, higher modulation schemes and multiple antennas are mandatory to attain the estimated performance levels within the power and bandwidth limitations. In this chapter, we study the modulation techniques used and the characteristics of a wireless channel in detail.

At the FEC block, redundancy is added to the information sequence in order to reduce the errors induced by the noisy channel. The FEC schemes used in our simulations are studied in Chapter 4. At the decoding stage, the soft outputs (LLRs) from the MIMO decoder

block are given as inputs to the channel decoder. As mentioned, fixed BWA systems face two key challenges which are, to provide high-data-rate and high-quality wireless access over fading channels at almost wireline quality. The use of multiple antennas (spatial diversity) at the transmit and receive sides of a wireless link in combination with signal processing and coding is a promising means to meet all these requirements [4]. The benefits provided by the use of multiple antennas at both BS and SS are array gain, diversity gain, interference suppression and multiplexing gain [4]. The major MIMO techniques, space-time-block codes [8] and spatial multiplexing [9], are studied in detail in Chapter 3.

2.3 Digital Modulation Schemes

Generally most natural signals like voice and music are centered at frequencies relatively close to zero. Before transmission in a wireless system, these lowpass (baseband) signals have to be converted to bandpass signals by moving the frequency content to be centered at a frequency $f_c \gg 0$. This process is called modulation. Modulation is required because, low frequency transmission would require enormous antennas which is not feasible. Low frequency band is the home for many man-made noises which might effect the desired signal. Also because of the broadcast nature of the wireless channel, natural frequency signals might overlap and cause interference. The primary measure of performance of a digital modulation scheme is the bit-error-rate (BER) which is nothing but the probability of a bit received as an error. The goal of a communication system design should be to reduce this BER in the available power and bandwidth [10].

2.3.1 Representation of Communication Signals

Any bandpass signal for most modulation types can be represented as

$$s(t) = \text{Re}\{s_l(t)e^{j2\pi f_c t}\} \quad (2.1)$$

Where $s_l(t) = x_r(t) + jx_i(t)$ is the complex information-bearing portion of the signal. In digital modulation, $x_r(t)$ and $x_i(t)$ are chosen from a fixed set of M possible signals that are

known to the transmitter and receiver. The m -th signal can be written as

$$s_m(t) = x_{r,m}\phi_1(t) + x_{i,m}\phi_2(t) \quad 0 \leq t \leq T_s; \quad m = 1, 2, \dots, M-1 \quad (2.2)$$

where

$$\begin{aligned} \phi_1(t) &= \sqrt{\frac{2}{T_s}}g(t) \cos 2\pi f_c t \\ \phi_2(t) &= -\sqrt{\frac{2}{T_s}}g(t) \sin 2\pi f_c t \end{aligned}$$

$x_{r,m}, x_{i,m} \in \mathbb{R}$ and $g(t)$ is essentially a bandwidth and time limited pulse known to the transmitter and receiver. The transmitted information is carried in the complex number $x_{r,m} + jx_{i,m}$, which is typically called a symbol. Typically $M = 2^p$ for some integer p , so that we can assign μ bits to each signal, yielding a transmission rate of $\log_2 M$ bits per time T_s . The scale factor $\sqrt{\frac{2}{T_s}}$ and $g(t)$ are chosen to ensure that $\phi_1(t)$ and $\phi_2(t)$ are orthonormal which means that they should be orthogonal and have unit energy [10].

The different modulation techniques supported by the IEEE 802.16-2004 standard are spread BPSK, BPSK, QPSK, 16-QAM, 64-QAM and 256-QAM. In our final results and simulations, QPSK is used and hence we elaborate on PSK in the next section.

2.3.2 M-ary Phase Shift Keying (MPSK)

BPSK and QPSK stand for binary and quadrature phase shift keying respectively. Binary digital modulation involves transmission of one signal for a binary 1 and a different signal for binary 0. In BPSK, we set $M = 2$, $x_{r,1} = \sqrt{E_s}$, $x_{r,2} = -\sqrt{E_s}$, $x_{i,1} = 0$, $x_{i,2} = 0$. So, to represent the bits 1 and 0 over the symbol interval T_s , we transmit

$$s_1(t) = \sqrt{E_s}\phi_1(t)$$

$$s_2(t) = -\sqrt{E_s}\phi_2(t)$$

respectively over $0 \leq t \leq T_s$. Where $g(t)$ can be any unit energy pulse that satisfies Nyquist's criterion for zero inter symbol interference (ISI). Often $g(t)$ will be a sinusoid

such as $\cos(2\pi f_c t)$. When $g(t)$ is a sinusoid, $s_1(t)$ and $s_2(t)$ differ by a phase shift π , hence the name binary phase-shift keying. E_s represents the transmitted signal energy per symbol. M-ary PSK is created by adding phase shifts other than π . The general expression for MPSK is

$$x_{r,m} = \sqrt{E_s} \cos \left[\frac{2\pi}{M}(m-1) \right] \quad m = 1, 2, \dots, M-1 \quad (2.3)$$

$$x_{i,m} = \sqrt{E_s} \sin \left[\frac{2\pi}{M}(m-1) \right] \quad (2.4)$$

This yields

$$s_m(t) = \sqrt{\frac{2E_s}{T_s}} g(t) \cos \left[2\pi f_c t + \frac{2\pi}{M}(m-1) \right] \quad (2.5)$$

In the case of QPSK, $M = 4$ and $p = 2$. So each of the four possible transmitted signals is assigned to one of the bit pairs 00, 01, 10, or 11 and the rate is 2 bits per symbol interval. Notice that as M increases, the number of bits per symbol increases, but the bandwidth of the transmitted signal does not change. Although the bandwidth efficiency improves with increasing M, the energy efficiency degrades as M increases [10].

2.3.3 Constellation Mapping

The FEC code bits are mapped to the I and Q symbol co-ordinates using Gray code mapping as shown in the Fig. 2.2 depending upon whether BPSK or QPSK is used. In Gray encoding, the messages associated with signal amplitudes that are adjacent to each other differ by one bit value. With this encoding, when the receiver makes a mistake in estimating the transmitted symbol to its adjacent one (most likely), the result is only a single bit error in the sequence of K bits [11].

The points in the constellation are symbols. For BPSK, they are $\sqrt{E_s}$ and $-\sqrt{E_s}$ and for QPSK, the four symbols can be found as $\{-\sqrt{E_s}, \sqrt{E_s}, -j\sqrt{E_s}, j\sqrt{E_s}\}$ or $\left\{ \sqrt{\frac{E_s}{2}} + j\sqrt{\frac{E_s}{2}}, \sqrt{\frac{E_s}{2}} - j\sqrt{\frac{E_s}{2}}, -\sqrt{\frac{E_s}{2}} + j\sqrt{\frac{E_s}{2}}, -\sqrt{\frac{E_s}{2}} - j\sqrt{\frac{E_s}{2}} \right\}$ These modulated symbols are transmitted

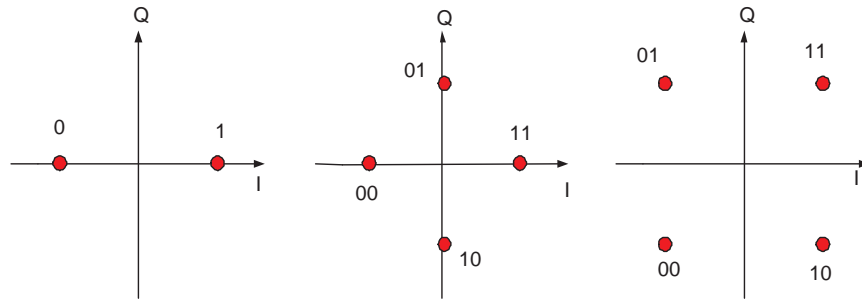


Figure 2.2: Constellation mapping for BPSK and QPSK with Gray encoding.

through the wireless channels possibly from multiple antennas. The nature of the wireless channel and the ways in which the transmitted signal gets distorted while passing through this channel is studied in the next section [10].

2.4 Wireless Channel

In the design of a wireline communication system, the primary source of noise is the thermal noise at the receiver front end and hence channel can be modeled as additive white Gaussian noise (AWGN). However, such model is not appropriate for a wireless channel because of its challenging physical nature due to which the signal has to undergo mechanisms such as path loss, reflection, scattering and diffraction. Some of the factors that influence fading are multipath propagation, speed of the mobile, speed of the surrounding objects and transmission bandwidth of the signal. The signals are subject to both large and small scale fading introduced by the channel. As the distance between the transmitter and receiver increases, the received signal power varies gradually at a large scale which is termed large scale fading and includes path loss and shadowing [12]. On the other hand, the rapid fluctuations of amplitude, phase and multipath delays of a radio signal over short period of time or distances is termed small scale fading. These multipath components at the receiver might combine sometimes constructively and sometimes destructively which causes distortion of the signal [10].

In our simulations, we ignore the large scale fading effects and only take small scale fading into consideration. There are different categories of small scale fading. Based on multipath

time delay spread, the transmitted signal undergoes either flat fading or frequency selective fading and based on Doppler spread the signal undergoes either fast or slow fading. The signal undergoes flat fading when the bandwidth of the signal is less than the coherence bandwidth of the channel or equivalently, if the symbol period is greater than the multipath spread. Under these conditions, the received signal has amplitude fluctuations due to the variations in the channel gain over time caused by multipath. However, the spectral characteristics of the transmitted signal remain intact at the receiver. On the other hand the signal undergoes frequency selective fading when the coherence bandwidth of the channel is much less than the bandwidth of the transmitted signal or equivalently, if the symbol period is less than the multipath spread. In this case, the received signal is distorted and dispersed, because it consists of multiple versions of the transmitted signal, attenuated and delayed in time. This leads to time dispersion of the transmitted symbols within the channel arising from these different time delays resulting in intersymbol interference (ISI). A channel is classified as slow fading if channel variations are much slower than the baseband signal variations or equivalently, if the coherence time of the channel is much larger than the symbol period. A signal undergoes fast fading if the symbol duration is larger than the coherence time of channel.

2.4.1 Rayleigh Fading Distribution

The complex-baseband received signal in a multipath fading channel can be modeled as

$$r_l(t) = \sum_{n=1}^L \alpha_n(t) e^{-j2\pi f_c \tau_n(t)} s_l(t - \tau_n(t)) \quad (2.6)$$

Where L is the number of paths, $\{\alpha_n(t)\}_n$ and $\{\tau_n(t)\}_n$ are the attenuation factor and propagation delay respectively. These two fading parameters are modeled as random processes as they keep varying and are not deterministic in nature. The delays are often considered to be uniformly distributed over a reasonable number of symbol periods. Rayleigh fading distribution is a kind of probability distribution used to model the received signal envelope, which is determined by $\{\alpha_n(t)\}_n$. This model is used for channels that do not have a strong LOS component. It assumes a large number of scatterers so that the central limit

theorem leads to a Gaussian distribution for the fading coefficients. The fading coefficient can be written as

$$\alpha(t)e^{-j2\pi f_c \tau(t)} = x_a(t) + jy_a(t) \quad (2.7)$$

where $x_a(t)$ and $y_a(t)$ are independent zero mean (because there is no strong line of sight component) real Gaussian random processes. In such case, $\sqrt{x^2 + y^2}$ has a Rayleigh distribution and hence the received signal envelope, $\alpha(t)$ has a Rayleigh distribution with its phase uniformly distributed over $[0, 2\pi)$.

2.4.2 Block Fading

One of the simplest fading models for time varying channels is block fading [13]. Here, the fading coefficients are modeled as constant over a block of symbols and vary independently between blocks. The simulation becomes extremely simple because of the lack of correlation among any fading coefficients. The received signal after lowpass filtering for a block consisting of N symbols with duration T can be written as

$$r_l(t) = hs_l(t) + n(t), \quad 0 < t \leq NT \quad (2.8)$$

where $s_l(t)$ is the baseband transmitted signal and $h \in \mathbb{C}$ is a random variable drawn from a complex Gaussian distribution. Notice that h does not change during the block and hence this model can be used for slow fading channels.

2.4.3 Performance of BPSK and QPSK

The analytical expression for the probability of bit error in AWGN channel for BPSK or QPSK modulation is given by $Q(\sqrt{\frac{2E_b}{N_0}})$, with $\frac{E_b}{N_0} = \gamma$ being the signal-to-noise ratio. The BER expression for a fading channel can be evaluated by averaging the error in AWGN channel over the fading probability density function as

$$P_e = \int_0^\infty P_e(\gamma)p(\gamma)d\gamma \quad (2.9)$$

where $P_e(\gamma)$ is the probability of error at a specific value of signal-to-noise ratio (SNR) γ and $p(\gamma)$ is the probability density function of γ of the fading channel. If we consider a unity gain fading channel, $p(\gamma)$ is simply the distribution of the instantaneous SNR in a fading channel. Whereas for Rayleigh fading channels, the fading power $|h|^2$ and hence the SNR γ have an exponential distribution given as

$$p(\gamma) = \frac{1}{\gamma_0} \exp\left(-\frac{\gamma}{\gamma_0}\right) \quad (2.10)$$

where $\gamma_0 = \frac{E_b}{N_0}|h|^2$ is the average SNR. Therefore the average BER in a Rayleigh fading channel can be calculated as

$$\bar{P} = \int_0^{\infty} Q(\sqrt{2\gamma}) \frac{1}{\gamma_0} \exp\left(-\frac{\gamma}{\gamma_0}\right) d\gamma \quad (2.11)$$

The above equation can be evaluated to [14]

$$\bar{P} = \frac{1}{2} \left[1 - \sqrt{\frac{\gamma_0}{1 + \gamma_0}} \right] \quad (2.12)$$

The BER equations exhibit an inverse algebraic relation between error rate and SNR for a Rayleigh fading channel and an exponential relationship for an AWGN channel. The BER curves for AWGN and Rayleigh fading channels are shown in Fig. 2.3. We can observe that the BER performance in a Rayleigh fading channel is very poor compared to AWGN channel. For example, an SNR of 24 dB is required to achieve a BER of 10^{-3} in the Rayleigh fading channel which is achieved with 3 dB SNR in the AWGN channel. This poor performance can be attributed to deep fades and in such environments the performance can be significantly improved by diversity techniques and error control coding which we will study in the later chapters.

2.5 Summary

WiMax primarily operates in two frequency bands: 10-66 GHz for LOS and below 11 GHz for NLOS. The features of WirelessMAN-SCa PHY are described. The wireless channel is

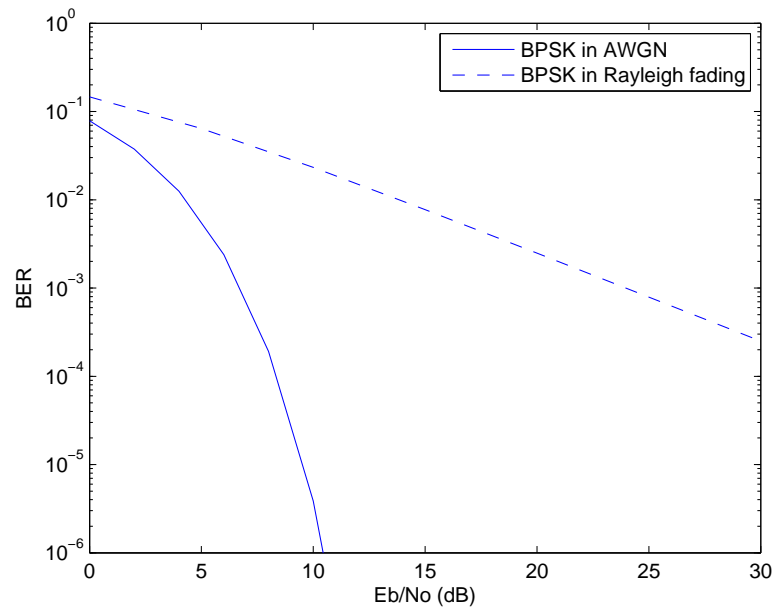


Figure 2.3: SNR vs BER for BPSK in AWGN and fading.

effected by small and large scale fading. Small scale fading can be flat or frequency selective and slow or fast. The representation of signals in a flat and slow varying channel is described. The wireless channel is modeled as a block Rayleigh fading channel. The phase-shift-keying modulation scheme is studied and the signal degradation in a fading channel compared to an AWGN channel is shown through simulation results.

Chapter 3

Multiple Antenna Systems

3.1 Introduction to Diversity

The two key issues in the physical layer level design of wireless communication are fading due to multipath propagation and interference of external signals. When a signal is transmitted in a fading channel, the signals travel in multiple paths from the transmitter to the receiver. These multiple versions of the transmitted signal, which will vary in their amplitudes and phases as they go through different paths of the channel, can combine either constructively or destructively at the receiver. The parameters like amplitude and phase of these signals also varies very rapidly even with small movements of the transmitter or receiver. Therefore fading leads to unreliable communication links. Interference can be of several forms. Self interference is caused from reflected copies of the desired signal. Co-channel interference is caused from other users of the same wireless network. External interference is caused due to wireless signals originating outside the network. To build a good wireless system we need to combat both fading and interference.

Diversity is a technique to combat fading and mitigation for interference. Diversity improves the reliability of the wireless system by exploiting the multipath propagation property of the radio channel. As in most of the wireless systems, the multiple copies of the received signal are affected by independent fading phenomenon and the chances of reliable reception is greatly increased at the receiver by making use of diversity techniques. The possible forms of diversity are time diversity, frequency diversity, path diversity and antenna diversity. As

the fading levels change with time, we can transmit the same signal at different times to achieve time diversity. Forward error correction (FEC) coding and rake reception of spread-spectrum signals may be considered as time diversity. A rake receiver anticipates multipath propagation delays of the transmitted spread spectrum signal and combines the information obtained from several resolvable multipath components to form a stronger version of the signal [14]. Transmitting the signal at different frequencies forms frequency diversity, spread-spectrum techniques and OFDM are forms of frequency diversity. Sending the signals over the wireless channel in many different paths forms path diversity. Transmitting or receiving the signal through multiple antennas at slightly different locations forms antenna diversity.

The original signal can be recovered by making use of the information of the desired signal and the interference. The three widely used methods to mitigate interference are designing a receiver which makes the optimum decision, the maximum a posteriori (MAP) equalizers or maximum likelihood sequence equalizer (MLSE) which are very complex. The second method to mitigate interference is to decorrelate the signal from the interference and the third method is to estimate the interference and subtract it out. Same as diversity, interference mitigation techniques can be performed in time, frequency or space [15].

3.1.1 Diversity Combining Techniques

Diversity combining of independently faded signals is a technique used at the receiver to mitigate the effects of fading. Here the fact that the signal-to-noise ratio (SNR) of the combined signals at the receiver is more than that of the individual branch SNR is considered. Diversity techniques allow the receiver several chances to determine the correct signal. As many replicas with a slight change in amplitude and/or phase of the original signal are available at the receiver, the receiver has to process these signals in order to obtain the desired signal. There three ways of processing or combining the signals are equal gain combining, selection combining and maximal ratio combining [15].

Fig. 3.1 shows diversity combining at the receiver. $s(t)$ is the transmitted signal which is received as $r(t)$ at the receiver through various independent paths. α_1 and α_2 are the

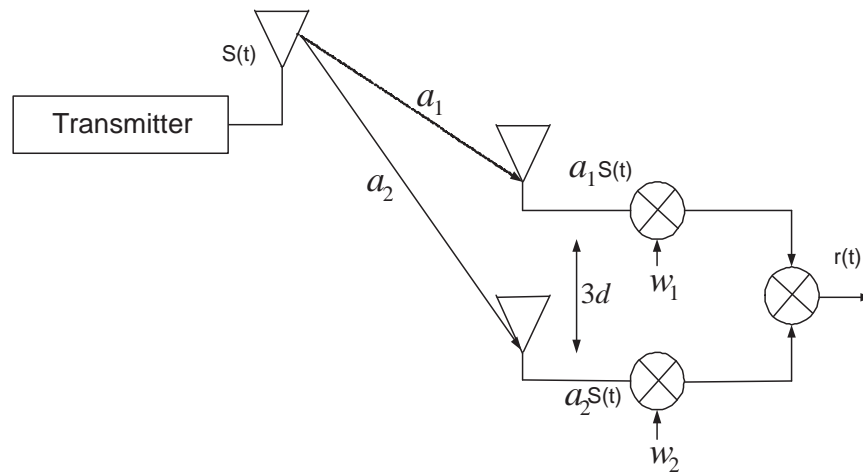


Figure 3.1: Diversity Combining at the Receiver.

fading coefficients of the two paths respectively. They can either be Rayleigh or Ricean depending upon the presence of the line of sight. The distance between the antennas should be a minimum of $3d$, where d is the wavelength of the signal. The received signal $r(t)$ can be written as $r(t) = w_1 a_1 s(t) + w_2 a_2 s(t)$ where w_1 and w_2 are the weights that are chosen by the receiver to multiply with the signal on each of the diversity branch. Following diversity combining techniques tell us how to choose the weight w_l .

Maximal Ratio Combining

Maximal ratio combining (MRC) technique gives the best statistical reduction of fading of any known linear diversity combiner and is the optimal one [14]. MRC improves on other diversity schemes by coherently combining each diversity branch to provide the largest possible SNR [10]. Assuming that there are L branches available, select weights w_1, \dots, w_L to maximize the SNR of the combined decision statistic $r = \sum_{i=1}^L w_i r_i$. we can interpret this as weighting each decision statistic in direct proportion to the relative strength of the signal component. We may use $w_l = |\alpha_l|$, $l = 1, \dots, L$. The instantaneous SNR of MRC can be written as

$$\gamma_{MRC} = \frac{E_s \sum_{l=1}^L |\alpha_l|}{N_0} \quad (3.1)$$

The average SNR for MRC is calculated as

$$\bar{\gamma}_{MRC} = E[\gamma_{MRC}] = \bar{\gamma} \cdot L \quad (3.2)$$

where $\bar{\gamma}$ is the average SNR. MRC does not throw away any energy even from the low SNR branches. Therefore, MRC coherently adds all available energy from all diversity branches, yielding the largest possible average SNR. The analytical expression of the probability of error for BPSK in the presence of L -branch diversity channel with MRC can be found by averaging the BER of BPSK in AWGN, given by $Q(\sqrt{2\gamma})$ over the distribution of SNR (γ) of MRC. The analytical expressions for BER with BPSK and QPSK in Rayleigh fading can be used to determine their performance [16]. For a L -branch channel they are calculated as

$$\bar{P}_{b,BPSK} = \frac{1}{2} \left[1 - \mu \sum_{l=0}^{L-1} \binom{2l}{l} \left(\frac{1 - \mu^2}{4} \right)^l \right], \mu = \sqrt{\frac{\gamma_0}{1 + \gamma_0}} \quad (3.3)$$

$$\bar{P}_{b,QPSK} = \frac{1}{2} \left[1 - \rho \sum_{l=0}^{L-1} \binom{2l}{l} \left(\frac{1 - \rho^2}{4} \right)^l \right], \rho = \frac{\mu}{\sqrt{2 - \mu^2}} \quad (3.4)$$

$$\gamma_0 = \begin{cases} \bar{E}_b/N_0, & \text{receive diversity} \\ \bar{E}_b/LN_0, & \text{transmit diversity} \end{cases}$$

In the Fig. 3.2, the lower curve indicates BPSK and higher curve QPSK. We can see that the slopes of the curves are the same for both BPSK and QPSK for a particular branch. The shift in the curve shows the coding gain where as the identical slope denotes that there is no diversity improvement between BPSK and QPSK. Since MRC gives the optimal performance by increasing the slope of the SNR-BER curve, it serves as a good reference for comparison with any other diversity scheme. Therefore, a system whose BER curve has the same slope as MRC but perhaps shifted to the right with L -branches is said to exploit full L -branch diversity [10].

Selection Combining

The conventional selection combiner(CSC) selects the signal from that diversity branch which has the largest instantaneous SNR, i.e. only the strongest decision statistic is used

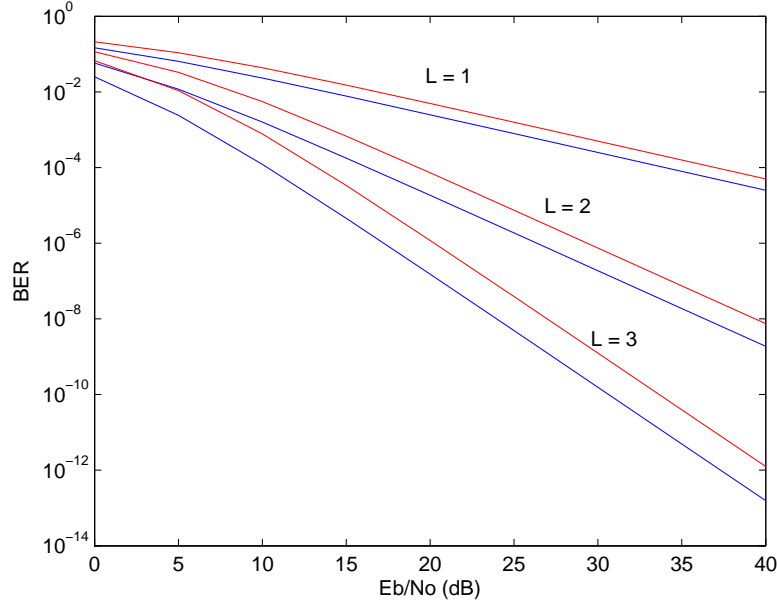


Figure 3.2: Bit error rate of BPSK (lower curve) and QPSK (higher curve) in a fading channel for $L = 1, 2, 3$ with MRC decoding

to compute the answer. The receiver simply decodes the branch with the largest SNR and ignores the other branches.

$$w_l = \begin{cases} 1, & \text{if } |\alpha_l| > |\alpha_j|, \forall j \neq l \\ 0, & \text{else} \end{cases} \quad (3.5)$$

Which means the instantaneous SNR of selection diversity can be written as

$$\gamma_{SD} = \frac{E_s \max_l |\alpha_l|}{N_0} \quad (3.6)$$

So that the average SNR can be written as where E_s is the symbol energy and N_0 is the noise power of the signal.

$$\bar{\gamma}_L = E[\gamma_{SD}] \quad (3.7)$$

which evaluates to

$$\bar{\gamma}_L = \bar{\gamma} \left(1 + \sum_{l=2}^L \frac{1}{l} \right) \quad (3.8)$$

where $\bar{\gamma}$ is the average SNR on each individual branch, and $\bar{\gamma}_L$ is the average SNR for L branches. It can be clearly seen that $\bar{\gamma}_L > \bar{\gamma}$. It can also be seen that $\gamma_{SD} < \gamma_{MRC}$. According

to a paper written by Ning Kong [17], he proposed a generalized selection scheme (GSC) where instead of selecting only the largest instantaneous SNR diversity branch as in CSC, m largest signals from L total diversity branches are selected and then coherently combined. The average SNR of this GSC is found to be upper bounded by the average SNR of the optimal diversity combining scheme MRC and lower bounded by the average SNR of CSC scheme. The selection diversity scheme is not the best as the receiver throws away energy from all other diversity branches other than the one with the largest SNR [17]. This is a good choice when the signals fade independently where at least one signal will be strong and usable.

Equal Gain Combining

Here equal gain weights are chosen i.e. $w_l = 1$, for $l = 1, \dots, L$ where L is the number of branches. Therefore all the branches are taken into consideration by giving them unity weights. The received signal will be of the form $r(t) = \alpha_1 s(t) + \alpha_2 s(t)$ when $L = 2$ and the receiver will decode this signal. This is a good technique to use when we know that all the components are equally distributed. In the other case when there are weak components present along with the strong components on different branches, giving them equal weights is not a good idea. Because the weak components might contribute a lot of noise than signal information to the overall decision statistic for the receiver to decode the signal.

3.2 MIMO Techniques

Multiple-input-multiple-output (MIMO) systems employ transmit diversity combined with receive diversity and allows us to explore both fading and interference problems. The primary reason for the extensive research on multiple antennas is that spatial diversity can typically be exploited without the bandwidth expansion. The multiple antennas can be used to increase the data rates through multiplexing or to improve performance through diversity [11].

Diversity was studied in the previous section. Transmit diversity is more favorable since the complexity is moved to the base station where more space or energy is available. Water-

filling [18] can be approached if feedback of the channel is available at the transmitter but this can also be a disadvantage as the complexity increases. The other disadvantage with transmit diversity is that it suffers a power penalty because the energy must be divided between multiple antennas. Multiplexing exploits the structure of the channel gain matrix to obtain independent signaling paths that can be used to send independent data [9]. Since MIMO techniques improve the data rate and reliability of wireless communication by providing diversity advantage and coding gain through multiplexing, they are being employed on almost all the PCS towers, WiFi base stations, WiMAX base stations. MIMO systems can offer many times the throughput of conventional SISO wireless links without increasing the transmitted power or bandwidth. The two categories of MIMO systems are space-time trellis code (STTC) [19] and space-time block code (STBC) [8]. Both the schemes are types of encoding procedures at the transmitter. The main goal of STBC is to obtain diversity advantage where as that of STTC is both diversity advantage as well as coding gain which makes the STTC system more complex than the STBC. Some hybrid schemes such as BLAST [20] approach are also possible in which the emphasis is signal processing at the receiver. The goal of these hybrid schemes is to achieve high data rates which makes them more complex. They are discussed in detail in the further sections [15].

There are several questions regarding space time codes that demand our attention. The first question is whether space time coding can achieve the same diversity advantage as MRC. The second question is can coding gain also be achieved in addition to diversity advantage and how much bandwidth efficiency does these schemes provide [21]. The answers to these questions are obtained by further detailed study.

3.2.1 Space-Time Block Codes

As a naive space time coding approach, we transmit the same data through the available number of transmit antennas suppose for example two transmit antennas and one receive antenna. After matched filtering, the received discrete-time signal at the single receive antenna will be of the form

$$r = \frac{1}{\sqrt{2}}(\alpha_0 + \alpha_1)s + n \quad (3.9)$$

Where s is the transmitted symbol, α_0, α_1 are the complex Gaussian channel coefficients on the two paths between the receive antenna and transmit antennas 1 and 2, respectively, and n is additive Gaussian noise. Since we are sending the same symbol from the two transmit antennas, we have to divide the power among the two antennas, hence the square root factor. At the receiver we multiply the received signal by $(\alpha_1 + \alpha_2)^*$, which yields the decision statistic

$$y = \frac{1}{\sqrt{2}}|\alpha_0 + \alpha_1|^2 b + v \quad (3.10)$$

Where v is still a Gaussian noise sample. To determine the performance of this system, we need to compare the pdf of the SNR to that of the 2-branch MRC. However, the distribution of $\frac{1}{\sqrt{2}}(\alpha_0 + \alpha_1)$ is same as the distribution of α_0 or α_1 alone. Therefore we get no diversity gain by this method of sending the same data from the available number of antennas [10].

Orthogonal space-time block codes with n_T transmit antennas and n_R receive antennas are coding strategies that provide full $n_T.n_R$ diversity with little or no rate penalty. The first example code of such kind is the Alamouti space time block code [8]. This two transmit antenna code provides full $2.n_R$ diversity with no rate penalty and very simple decoding. Suppose we wish to transmit two symbols s_0 and s_1 over a flat fading channel with two transmit antennas and one receive antennas (the example can be easily extended to more receive antennas). Ideally, we would like to achieve a 2-branch MRC performance. We have seen that transmitting each symbol separately from both antennas provides no transmit antenna diversity gain. The Alamouti space time block code [8] matrix is

$$\mathbf{S} = \begin{bmatrix} s_0 & s_1 \\ -s_1^* & s_0^* \end{bmatrix} \quad (3.11)$$

where the row indicates the symbols transmitted from the two transmit antennas during the first time slot, and the second row indicates the symbols transmitted during the second time slot. The discrete-time received signal at antenna 1 during the two symbol intervals is

$$r_0 = \alpha_0 \frac{s_0}{\sqrt{2}} + \alpha_1 \frac{s_1}{\sqrt{2}} + n_0 \quad (3.12)$$

$$r_1 = -\alpha_0 \frac{s_1^*}{\sqrt{2}} + \alpha_1 \frac{s_0^*}{\sqrt{2}} + n_1 \quad (3.13)$$

where the square root factor is needed to ensure unit transmit power for each symbol. The noise samples n_0 and n_1 are independent and identically distributed complex Gaussian zero-mean random variables with power N_0 . The estimates of the symbols at the receiver are given by

$$\tilde{s}_0 = \alpha_0^* r_0 + \alpha_1 r_1^* = \frac{1}{\sqrt{2}}(|\alpha_0|^2 + |\alpha_1|^2)s_0 + \alpha_0^* n_0 + \alpha_1 n_1^* \quad (3.14)$$

$$\tilde{s}_1 = \alpha_1^* r_0 - \alpha_0 r_1^* = \frac{1}{\sqrt{2}}(|\alpha_0|^2 + |\alpha_1|^2)s_1 + \alpha_1^* n_0 - \alpha_0 n_1^* \quad (3.15)$$

The instantaneous SNR for each symbol is

$$\frac{|\alpha_0|^2 + |\alpha_1|^2}{2N_0} \quad (3.16)$$

This system provides the same diversity performance as 2-branch MRC, although there is a 3 dB SNR loss caused by the fact that we must split the transmit power across two transmit antennas. Notice also that the Alamouti scheme transmits two symbols in two time slots. Therefore the rate of the code is 1, which means there is no loss of bandwidth to achieve full transmit antenna diversity. The Alamouti scheme [8] works because the columns of the space-time block code matrix are orthogonal. A natural question to ask is, do space-time block code matrices exist for more than two transmit antennas? The answer is yes, but with qualifications. For complex symbols, there are no full-rate space-time block code matrices for more than two transmit antennas. Tarokh [22] provided examples of lower rate code matrices that provide full diversity.

Generalized Real Orthogonal Designs

A generalized real orthogonal design is a $p \times n_T$ matrix \mathbf{G} with entries $0, \pm x_1, \pm x_2, \dots, \pm x_k$ such that $\mathbf{G}^T \mathbf{G} = (x_1^2 + x_2^2 + \dots + x_k^2) \mathbf{I}_{n_T \times n_T}$. p represents the delay required by the code. The goal in the design of real STBC is to design a code that achieves full diversity $n_T n_R$ for a given number of transmit antennas n_T and a given rate $R = k/p$. Because p represents delay and lowers rate, the goal is to find designs which minimize p . Tarokh's paper [22] provides \mathbf{G} for generalized real orthogonal designs for $n_T = 1, \dots, 8$ and that have rate $R = 1$.

Generalized Complex Orthogonal Designs

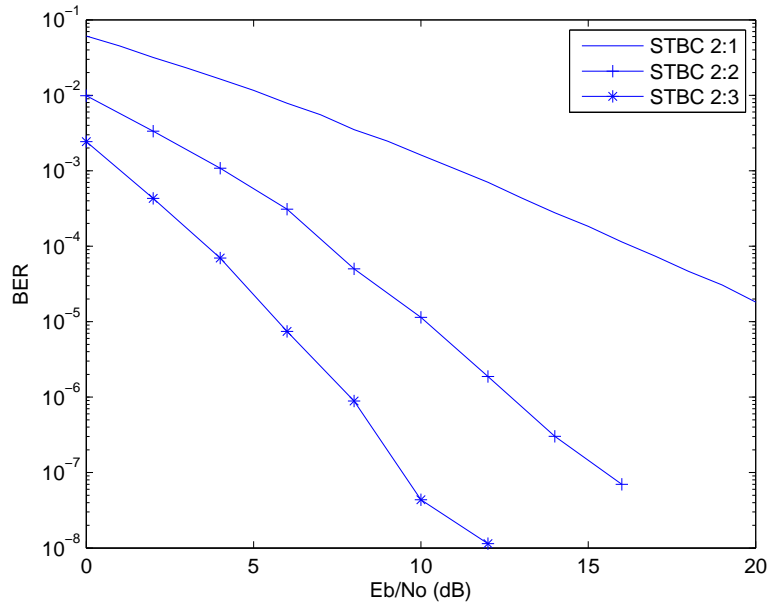


Figure 3.3: Alamouti space time block code with QPSK in Rayleigh fading channel with MRC decoding.

A generalized complex orthogonal design is a $p \times n_T$ matrix \mathbf{G} with entries $0, \pm x_1, \pm x_2, \dots, \pm x_k, \pm x_1^*, \pm x_2^*, \dots, \pm x_k^*$ such that $\mathbf{G}^\dagger \mathbf{G} = (|x_1|^2 + |x_2|^2 + \dots + |x_k|^2) \mathbf{I}_{n_T \times n_T}$. Again one goal of the code design is to minimize the required delay p to achieve full-diversity code. Tarokh's paper [22] presents designs \mathbf{G} for rate 1/2 and rate 3/4 codes which achieve full diversity. There do not appear to exist full-rate complex orthogonal design codes for more than 2 antennas. For example if we have 3 transmit antennas and complex symbols, we can use the matrix,

$$\begin{bmatrix} s_0 & s_1 & s_2 \\ -s_1 & s_0 & -s_3 \\ -s_2 & s_3 & s_0 \\ -s_3 & -s_2 & s_1 \\ s_0^* & s_1^* & s_2^* \\ -s_1^* & s_0^* & -s_3^* \\ -s_2^* & s_3^* & s_0^* \\ -s_3^* & -s_2^* & s_1^* \end{bmatrix} \quad (3.17)$$

This scheme transmits 4 complex symbols over 3 antennas over 8 time slots. The columns

are orthogonal, so full transmit antenna diversity with linear ML decoding, but the normalized rate is $1/2$, instead of 1, as in the Alamouti 2 transmit antenna scheme [8]. Similar rate $1/2$ code matrices can be formed for four and more transmit antennas. Tarokh also provided a few known special cases of higher rate codes (rate $3/4$) for 3 and 4 transmit antennas. If the modulation symbols are real, there exists full rate orthogonal space-time block code matrices only for 2, 4, and 8 transmit antennas. For 4 transmit antennas, we can use

$$\begin{bmatrix} s_0 & s_1 & s_2 & s_3 \\ -s_1 & s_0 & -s_3 & s_2 \\ -s_2 & s_3 & s_0 & -s_1 \\ -s_3 & -s_2 & s_1 & s_0 \end{bmatrix} \quad (3.18)$$

The design goals are to achieve full diversity $n_T n_R$ where n_T and n_R are the number of transmit and receive antennas respectively, to achieve full rate $R = 1$, to minimize delay p and linear complexity at the receiver. For real constellations it is possible to achieve all these goals upto 8 antennas where as for complex constellations it is not possible to achieve full rate and full diversity for more than 2 antennas. It is possible to achieve rate $1/2$ and $3/4$ with full diversity for upto 4 antennas for complex constellations. Note that higher spectral efficiencies can be obtained even without full rate, by using larger signal constellations [15].

Note that there is no memory between consecutive blocks and that the typical block length is very short and thus a very limited coding gain is expected. The scheme has a very simple decoding structure and therefore it can be concatenated to a powerful outer error correction code. STBCs are limited in the number of transmit antennas that can be supported and still obtain an orthogonal design. At the decoupling stage, the combiner assumes that each received signal is composed by a linear superposition of current symbols corrupted by noise. This is not the case in high delay spread environment where there exists a strong channel-induced ISI component. Thus, the performance of STBC might be sensitive to such environments. Nevertheless, the scheme is still an appealing one for its simplicity and can be examined in conjunction with known techniques for e.g rake receiver [15].

3.2.2 Space-Time Trellis Coding

Space-time trellis codes (STTCs), are an extension of the conventional trellis codes to MIMO systems [19]. The criteria that have been primarily applied to the design of STTCs are the rank and determinant. They are described by a trellis diagram where this STTC maps k input bits and v state bits into n_T simultaneously transmitted symbols by using n_T generator polynomials. The decoding consists of channel estimation using ML sequence estimation via the Viterbi algorithm. The advantage of a well constructed STTC is that it achieves both diversity advantage and coding gain. The diversity advantage is the asymptotic slope of the error rate curves while coding gain is the offset in SNR from an uncoded system with same diversity advantage. Therefore, this STTC is a robust technique for a variety of mobility environments [19]. The major drawbacks are the complexity of the decoder increases exponentially with bandwidth efficiency in a STTC whereas STBC extracts excellent diversity gain which has much remarkably low decoder complexity. However, though STBCs achieve full diversity advantage, as they do not provide coding gain, their performance is inferior to that of STTCs which achieve both full diversity gain as well as coding gain. Added coding gain to STTCs as well as STBCs can be achieved by concatenating these codes either in serial or in parallel with an outer channel code. One more drawback is that there is a lack of general STTC constructions [19] [15].

3.2.3 BLAST Techniques

BLAST stands for Bell Labs layered space time architecture and was proposed by Foschini et al. from Bell labs [20]. It uses multiple transmit and receive antennas to obtain diversity by exploiting the rich scattering environment [9]. The transmitter transmits different sub channels through different antennas without including any orthogonality. The receiver uses sorting and multiuser detection technique to obtain the sub channels. The detailed procedure is studied in the coming sections. The channel assumptions for BLAST systems are that, the channel is known before hand and has a large number of multipath. The bandwidth is considered to be narrow well within the flat fading zone of the channel. A Quasi-static channel is assumed where the channel does not change significantly with in the symbol

duration. There are two types of BLAST techniques D-BLAST and V-BLAST.

D-BLAST

D-BLAST is a diagonal layered space time architecture in which coding is introduced between streams across diagonals in space-time. Here the data stream is first parallel encoded and rather than transmitting the codeword with one antenna, the codeword symbols are rotated across antennas, so that a codeword is transmitted by all the n_T transmit antennas present. As a result the codeword is spread across all spatial dimensions [15].

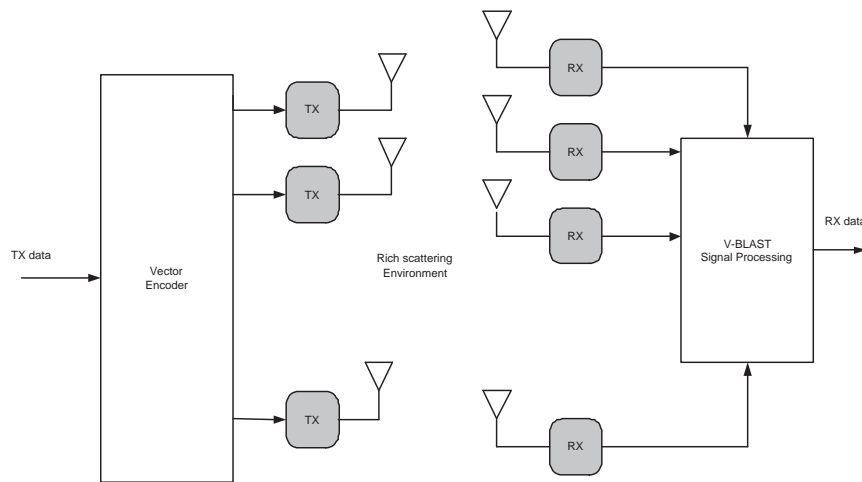


Figure 3.4: V-BLAST

V-BLAST

V-BLAST is considered to be the encoding of serial data into a vertical vector and hence referred to as vertical encoding. Thus, each antenna acts as a conventional transmitter with a single stream of data. It can achieve at most a diversity order of n_R , since each coded symbol is transmitted from one antenna and received by n_R antennas [20]. There are a number of schemes for the detection of V-BLAST that are relatively easy to implement and provide high performance.

- Original Algorithm (Zero Forcing, No-Ordering)
- Modified Algorithm (Zero Forcing, Optimal detection order)
- Maximum Likelihood Algorithm

Consider the number of transmit antennas to be n_T and receive antennas n_R . The transmitted data is represented in the form of a vector as $x = [x_1 x_2 x_3 \dots x_{n_T}]^T$ whose dimensions are $(n_T \times 1)$. The received vector will be of the form $r = Hx + v$ with dimensions $(n_R \times 1)$ where v is a complex Gaussian noise vector with zero mean and variance $\sigma^2(n_R \times 1)$ [15]. Channel matrix H with dimensions $(n_R \times n_T)$ is given as

$$H = \begin{bmatrix} h_{(1,1)} & \dots & h_{(n_T,1)} \\ \vdots & & \vdots \\ h_{(1,n_R)} & \dots & h_{(n_T,n_R)} \end{bmatrix} \quad (3.19)$$

The only difference between the original algorithm and modified algorithm is the selection of the first symbol to be decoded. In the modified decoding algorithm, first the strongest signal is decoded. Then, canceling the effects of this strongest symbol from all the received signals by considering the interference from all other symbols as noise, the algorithm detects the next strongest symbol. This way the algorithm continues by canceling the effects of the detected symbol and the decoding of the next strongest symbol until all the symbols are detected. This original algorithm works only when the number of receive antennas is more than that of the transmit antennas, that is $n_R \geq n_T$ [23]. The algorithm includes three steps

- ordering
- interference cancelation
- interference nulling

The purpose of ordering step is to decide which transmitted symbol to detect at each stage of the decoding. The symbol with highest SNR is the best pick in this step. The goal of interference cancelation is to remove the interference from the already detected symbols in decoding the next symbol. Finally, interference nulling finds the best estimate of a symbol from the updated equations. This step is called interference nulling since it can be considered as removing the interference effects of undetected symbols from the one that is being decoded. Zero-forcing(ZF) and Minimum mean-square error(MMSE) are the two types of nulling techniques. MMSE gives a better performance than ZF. Maximum likelihood algorithm makes a decision by considering only the closest neighbors in the constellation [23].

The main goal of BLAST systems is to substantially increase the throughput by using multiple antennas. This approach assumes that the number of receive antennas is greater

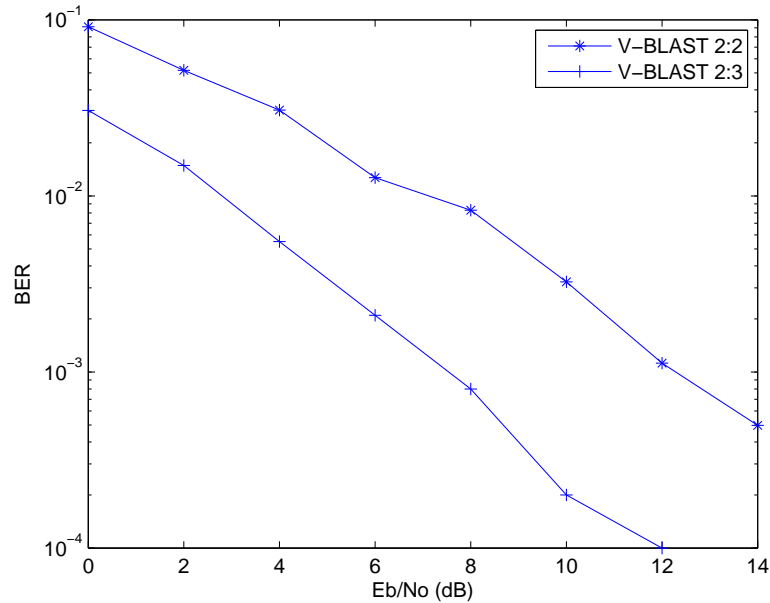


Figure 3.5: V-BLAST for QPSK using ML detector

than or equal to the number of transmit antennas. No orthogonality between the spatially separated signals is required at the transmitter and the channel should have rich scattering environment [15].

3.3 Summary

In this chapter, the methods to combat fading are explained by introducing the concept of diversity. Spatial diversity is taken as the point of interest and hence various diversity combining techniques used at the receiver end, to combine the multipath signals are studied and compared. It is concluded that MRC gives the optimal performance and hence any system with spatial diversity can be compared with MRC to evaluate its performance. Further, MIMO systems where spatial diversity is included both at the transmitter as well as the receiver are introduced. The two primary MIMO systems, STBCs and BLAST systems are studied in detail and their performances for different antenna configurations is plotted.

Chapter 4

Turbo Coding for WiMax

4.1 Channel Coding for WiMax-IEEE 802.16-2004

The WirelessMAN-SCa PHY supports several combinations of modulation and coding rates that can be used to achieve various trade-offs of data rate and robustness, depending on channel and interference conditions for both uplink and downlink. One of the FEC codes it supports is a concatenated FEC which uses an outer Reed-Solomon code (RS) [24] and an inner convolutional code [25] with optional interleaving between the outer and inner codes. The second FEC option is turbo coding which can be achieved either by a block turbo code (BTC) or a convolutional turbo code (CTC). Turbo coding can improve the coverage and/or capacity of the system, at the price of increased decoding latency and complexity [26]. Although the BTC and CTC are optional in the initial WiMax standards, they are made mandatory in the next and latest versions. There is also a no-FEC option supported by the standard where an automatic repeat request (ARQ) mechanism is used to transmit data reliably instead of FEC coding. In this project, we implement a convolutional turbo code as the FEC and further study the details of a turbo code in this chapter [5].

4.2 The need for Channel Coding

In 1948, Shannon demonstrated in a landmark paper [27] that, by proper encoding of the information, errors induced by a noisy channel can be reduced to any desired level without

sacrificing the rate of information transmission, as long as the information rate is less than the capacity of the channel. Therefore, coding for error control in a noisy environment is being used in almost all high speed communication systems [28]. Applying FEC coding in a wireless channel reduces the probability of bit error due to its error correction capability.

The amount of error reduction provided by a given code is typically characterized by its coding gain in AWGN and diversity gain in fading. Since FEC provides time diversity by adding redundancy to the data, we use it in addition to the multiple antennas which provides spatial diversity. Therefore, a channel code concatenated with MIMO, and with an appropriate modulation scheme, is proven to provide very good performance in a fading channel [11].

In Fig. 2.1, we see in the transmitter block that the modulator follows the channel encoder. The function of this channel encoder is to introduce, in a controlled manner, some redundancy in the binary information sequence, which can be used at the receiver to overcome the effects of noise and interference encountered in the transmission of the signal through the channel. The encoding process generally involves taking a k -bit sequence into a unique n -bit sequence, called a *code word* [16]. The amount of redundancy introduced by the encoding of the data in this manner is measured by the ratio n/k . The reciprocal of the ratio, k/n is called *code rate* [28].

At the receiver, the demodulator processes the signals which are impaired by the channel and reduces each signal to a scalar or vector that represents an estimate of the transmitted data symbol. The detector, which follows the demodulator, may decide on whether the transmitted bit is a 0 or a 1 ($M=2$). The detector quantizes the demodulator's metric to one of the quantization (Q) levels. The demodulator is said to make *hard decisions* when it has output quantization ($Q=2$ for $M=2$) in which case the decoder will have binary inputs. When the output of the demodulator is quantized to more than two levels, i.e. $Q > 2$ (or the output is left unquantized), the demodulator is said to make *soft decisions*. In this case, the decoder must accept multilevel or continuous valued inputs which makes its implementation difficult. Hard decisions in the demodulator result in some irreversible information loss as it discards information that can reduce probability of codeword error [29]. For example, in BPSK ($M=2$), the received symbol is decoded as 1 if it is closer to $\sqrt{E_b}$ and 0 if it closer to

$-\sqrt{E_b}$. Here, the distance of the received symbol from $\sqrt{E_b}$ and $-\sqrt{E_b}$ is not being used in decoding, yet this information can be used to make better decisions about the transmitted codeword. In soft decision decoding, the demodulator makes a soft decision corresponding to the distance between the received symbol and the symbol corresponding to a 0-bit or a 1-bit transmission [11]. In this chapter, the structure of the CTC which supports various frame sizes and code rates and the calculation of the soft values (LLRs) which are given as inputs to the decoder are studied.

4.3 Convolutional Turbo Coder

4.3.1 Introduction

Convolutional turbo codes [30], also called parallel concatenated convolutional codes (PCCC) were first introduced in 1993 by Berrou et al.. Today almost all the advanced FEC systems employing turbo codes are capable of achieving moderately low BERs of around 10^{-5} at SNRs within 1 dB of the Shannon limit [27] [28]. Turbo codes are proven to provide higher throughputs and higher data rates within the given power constraints.

4.3.2 CTC Encoder

The CTC encoder as depicted in the Fig. 4.1 has three main blocks, the constituent encoder, the interleaver and the puncturer. It uses a double binary circular recursive systematic convolutional code (CRSC) [31]. The term double binary implies that the encoder can accept two data bits per time instance and thus gives out four bits totally including the two systematic bits and the two parity bits. The CRSC encoding is performed in such a way that it should make sure that the initial and final states of the encoder are the same, which makes it circular. The CTC encoder can take in several frame sizes of information bits ranging from 32 bytes to 1024 bytes either in the form of E bits or F couples. As seen in Fig. 4.1, the polynomials defining the encoder connections are given as $1 + D + D^3$ for the feed back branch and $1 + D^2 + D^3$ for the Y parity bit. The information bits are fed through inputs A and B alternately starting with the most significant bit (MSB) of the first byte. In

the first step, A and B are directly taken as outputs also called systematic bits without any encoding and then they are fed into the constituent encoder 1 whose structure is shown in the figure. It gives out the parity bits Y_1 and W_1 . In the second step, the same information bit sequences A and B are passed through the interleaver and then the interleaved information bits are fed to the constituent encoder 2 which is similar to constituent encoder 1. This produces the parity bits Y_2 and W_2 . The final codeword can be formed as $ABY_1W_1Y_2W_2$. Since there are four parity bits and two systematic (data) bits, the code rate is $1/3$. Further code rates can be obtained by puncturing the code words [32] [5].

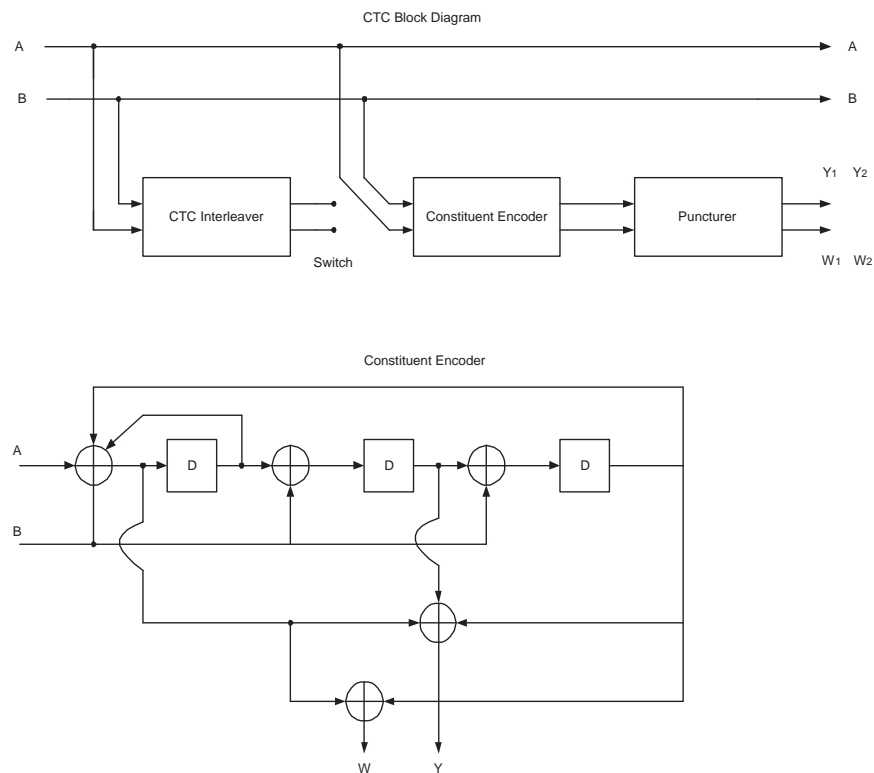


Figure 4.1: CTC encoder with a Constituent encoder.

The important aspect of the constituent encoder is attaining the circulation state S_c , where the initial and final states of the encoder are equal. In recursive encoding, this state is obtained by performing the following steps. First, encode the information sequence after initializing the encoder to all zeroes state and determine the final state in case of natural order and in case of interleaved order. In both the cases, this ending state is represented as S_N which is further used to calculate the circulation state S_c by some linear algebra methods

based on the state space description of the encoder. But alternately, the IEEE 802.16-2004 standard provides a circulation state look-up table shown in Fig. 4.2 to determine S_c based on S_N and the frame size N . Now after initializing the encoder to S_c determined from the look-up table, the information sequences are encoded again to obtain the parity bits. This time the encoder is guaranteed to end in state S_c as it is set to initially [33] [5]. Considering S_k as the state at time k which is represented by a 3 element column vector (8 possible states) containing the values stored in the D-flip flops in the Fig. 4.1, the encoder state at time k can be related to the state at time $k-1$ as

$$S_{k+1} = GS_k + X_k \quad (4.1)$$

and

$$Y = [1 \ 1 \ 0]S_{k+1} + [A_k + B_k] \quad (4.2)$$

where

$$X_k = \begin{bmatrix} A_k + B_k \\ B_k \\ B_k \end{bmatrix} \quad (4.3)$$

and

$$G = \begin{bmatrix} 1 & 0 & 1 \\ 1 & 0 & 0 \\ 0 & 1 & 0 \end{bmatrix} \quad (4.4)$$

4.3.3 CTC Interleaver

Interleaving the data along with coding increases the performance of the system. With a linear code, it is desirable to produce high weight codewords (e.g. codewords with a large number of 1's) because it is the lowest nonzero weight codeword that sets the minimum distance of the code and, hence, the error correcting capability of the code. Suppose that a particular message causes a low weight output from the constituent encoder 1, when the

N _{mod}	S _N							
	0	1	2	3	4	5	6	7
1	0	6	4	2	7	1	3	5
2	0	3	7	4	5	6	2	1
3	0	5	3	6	2	7	1	4
4	0	4	1	5	6	2	7	3
5	0	2	5	7	1	3	4	6
6	0	7	6	1	3	4	5	2

Figure 4.2: Circulation State Look up Table for IEEE 802.16-2004.

same message is interleaved and sent through the constituent encoder 2, it is not likely to also produce a low weight output. Thus, in a turbo code it is unlikely that both encoders simultaneously produce low weight outputs, and hence, the number of low weight codewords is very small, leading to the good performance of turbo codes. Before passing the information sequences A and B through the second encoder, the data is interleaved at two levels as follows

Step 1 : For every even value of j , i.e. if $(j_{mod_2} == 0)$ Interchange A_j and B_j , i.e. make $(A_j, B_j) = (B_j, A_j)$ where $j = 1, 2, \dots, N$. This is interleaving between the couples.

Step 2 : This step involves interleaving within the couples. Here we need a parameter P_0 which shall be the nearest prime number greater than $\sqrt{N/2}$. We compute the function $P_j(i)$ which gives the interleaved address i of the considered couple j . First, we calculate (j_{mod_4}) which can be 0, 2, 3 or 4. If 0 or 2, we get $i = (P_0 \cdot j + 1)_{mod_N}$ and if it is 3 or 4 we get $i = (P_0 \cdot j + 1 + N/4)_{mod_N}$ for $j = 1, 2, \dots, N$. The bits at the address positions j and i will be switched. These interleaved bits are fed to the second encoder [5] [33].

4.3.4 CTC Puncturer

The CTC puncturer selectively deletes parity bits in order to provide various code rates. The puncturing patterns to be followed are specified in the standard. To obtain code rates 1/2 and higher, all the W parity bits are deleted. For rate 1/2, all the Y parity bits are transmitted, for rate 2/3, every even indexed bit of Y is transmitted and for rates 3/4, 5/6,

and 7/8 every fourth, sixth and eighth bits are transmitted respectively [5] [33].

The order in which these encoded bits are given to the BPSK or QPSK symbol mapper is $A_0, B_0, \dots, A_{N-1}, B_{N-1}, Y_{10}, Y_{11}, \dots, Y_{1M}, Y_{20}, Y_{21}, \dots, Y_{2M}$ where, N is the information frame size and M is the Y parity bits block size for both interleaved and uninterleaved data. These bits are mapped according to the signal constellations shown in the third chapter [5].

4.4 CTC Decoder

The practical importance of turbo and serial concatenated codes lies in the availability of a simple suboptimum decoding algorithm [30]. Turbo decoding relies on the exchange of probabilistic information between the two soft-input soft-output (SISO) decoders [34]. Usually, and also in our implementation, the probabilistic information is expressed in the form of log likelihood ratio (LLR). The role of a SISO decoder consists of taking input LLR estimates of the transmitted bits and trying to improve these estimates by using the local redundancy of the considered component code [34]. The iterative decoders such as max-log-MAP [35] and log-MAP used in this project are based on maximum a posteriori probability (MAP) algorithm [34]. The detailed procedure to implement the CTC decoder can be seen in [33]. In this project implementation, the software used to simulate the CTC coded system leverages code developed at the Wireless Communications Research Laboratory (WCRL) and made available under the GPL license within the Iterative Solutions Coded Modulation Library (ISCML)¹. In the next section, the soft inputs or the LLRs to be given as inputs to the decoder are derived.

4.4.1 Calculation of the input LLRs to the decoder

The bitwise log likelihood ratios of the systematic bits and the parity bits are to be calculated at the output of the demodulation stage and given as inputs to the CTC decoder. In the implementation discussed here, we consider QPSK modulation, a 2×1 Alamouti space time block code [8], i.e. two transmitters and one receiver, Rayleigh fading channel

¹Iterative Solutions Coded Modulation Library, available at <http://www.iterativesolutions.com/Matlab.htm>, release 1.6.2 edition, July 2006

and MRC diversity combining at the receiver. The procedure to followed to calculate the bit LLRs is shown below.

The discrete signal model for a slow varying, flat fading channel can be written as

$$R = HS + N \quad (4.5)$$

where R is the received symbol vector, S is the transmitted symbol vector, $N \sim \mathcal{N}_c(0, \sigma^2 \mathbf{I})$ is the AWGN vector, and H the channel gain matrix given by

$$H = \begin{bmatrix} h_{11} & h_{21} \\ h_{21}^* & -h_{11}^* \end{bmatrix} \quad (4.6)$$

where h_{11} and h_{21} are the complex channel gains between the two transmit antennas and one receive antenna. The decision statistic 'd' at the receiver for MRC decoding is given by

$$d = H^H R \quad (4.7)$$

In a two transmit one receiver case,

$$s = \frac{1}{\sqrt{2}} \begin{bmatrix} s_1 \\ s_2 \end{bmatrix} \quad (4.8)$$

$$d = \begin{bmatrix} d_1 \\ d_2 \end{bmatrix} \quad (4.9)$$

d_1 and d_2 are calculated to be

$$d_1 = \frac{1}{\sqrt{2}} E_h s_1 + n_1 \quad (4.10)$$

$$d_2 = \frac{1}{\sqrt{2}} E_h s_2 + n_2 \quad (4.11)$$

where $E_h = |h_{11}|^2 + |h_{21}|^2$, n_1 and n_2 are the complex Gaussian noise with mean 0 and variance σ^2 . From equations of d we can see that, $\sigma_d^2 = E_h \sigma^2$. As described in the previous chapter, for QPSK modulation, we suppose $00 \rightarrow 1, 01 \rightarrow j, 11 \rightarrow -1, 10 \rightarrow -j$. From

this, we can describe the symbol sets $S_1^{(0)} = \{1, j\}$ is the set of symbols whose first bit is a 0, $S_1^{(1)} = \{-1, -j\}$ is the set of symbols whose first bit is a 1, $S_2^{(0)} = \{1, -j\}$ is the set of symbols whose second bit is a 0, $S_2^{(1)} = \{-1, j\}$ is the set of symbols whose second bit is a 1. The LLR for the k 'th bit of the i 'th symbol can be calculated as

$$\lambda_k(d_i) = \ln \left(\frac{\sum_{s \in S_k^{(1)}} P(s_i | d_i)}{\sum_{s \in S_k^{(0)}} P(s_i | d_i)} \right) \quad (4.12)$$

where $i = 1, 2$ for each estimated symbol. The equation of the LLR for the first bit of the first symbol d_1

$$\lambda_1(d_1) = \ln \left(\frac{P(s_1 = -1 | d_1) + P(s_1 = -j | d_1)}{P(s_1 = 1 | d_1) + P(s_1 = j | d_1)} \right) \quad (4.13)$$

$$= \ln \left(\frac{f(d_1 | s_1 = -1) + f(d_1 | s_1 = -j)}{f(d_1 | s_1 = 1) + f(d_1 | s_1 = j)} \right) \quad (4.14)$$

If $\lambda_1(d_1) > 0$, the first bit of $d_1 = 1$ or if $\lambda_1(d_1) < 0$, the first bit of $d_1 = 0$.

Similarly, the LLR for the second bit is given by

$$\lambda_2(d_1) = \ln \left(\frac{f(d_1 | s_1 = -1) + f(d_1 | s_1 = j)}{f(d_1 | s_1 = 1) + f(d_1 | s_1 = -j)} \right) \quad (4.15)$$

If $\lambda_2(d_1) > 0$, the second bit of $d_1 = 1$ or if $\lambda_2(d_1) < 0$, the second bit of $d_1 = 0$. By replacing d_1 with d_2 in the equation 4.15, we can find the bit LLRs for d_2 .

The conditional probability density functions (pdfs) in the equation 4.15 need to be calculated to get the value of LLRs. From the equations of d_1 and d_2 , we can see that d_1 depends only on s_1 and not on s_2 . Hence d_1 is the decision statistic for s_1 . Similarly d_2 is the decision statistic for s_2 . Consider the case when the first symbol $s_1 = 1$, we can write $d_1 = d_{1,r} + jd_{1,i}$ where $d_{1,r} = \frac{1}{\sqrt{2}}E_h + n_{1,r}$ is the real part and $d_{1,i} = n_{1,i}$ is the imaginary part with variance $\sigma_d^2 = E_h \sigma^2$.

$d_{1,r}$ is a Gaussian random variable with mean ' $\frac{1}{\sqrt{2}}E_h$ ' and variance ' σ_d^2 '. Therefore its pdf can be written as

$$f_{d_{1,r}}(d_{1,r} | s_1 = 1) = \frac{1}{\sqrt{2\pi}\sigma_d} \exp \left[\frac{-\left(d_{1,r} - \frac{1}{\sqrt{2}}E_h\right)^2}{2\sigma_d^2} \right] \quad (4.16)$$

$d_{1,i}$ is a Gaussian random variable with mean '0' and variance ' σ_d^2 '. So its pdf will be

$$f_{d_{1,i}}(d_{1,i}|s_1 = 1) = \frac{1}{\sqrt{2\pi}\sigma_d} \exp\left[-\frac{(d_{1,i})^2}{2\sigma_d^2}\right] \quad (4.17)$$

The Conditional pdf of d_1 given $s_1 = 1$ is given as

$$f_{d_1}(d_1|s_1 = 1) = f_{d_{1,r}}(d_{1,r}|s_1 = 1) \cdot f_{d_{1,i}}(d_{1,i}|s_1 = 1) \quad (4.18)$$

$$= \left(\frac{1}{2\pi E_h \sigma^2}\right) \exp\left[-\frac{\left|d_1 - \frac{1}{\sqrt{2}}E_h\right|^2}{2\sigma^2 E_h}\right] \quad (4.19)$$

Similarly the conditional pdfs $f(d_1|s_1 = -1)$, $f(d_1|s_1 = j)$, $f(d_1|s_1 = -j)$ are calculated and substituted in the equation to find out the bit LLRs. These LLRs for the whole codeword at the output stage of the demodulator are calculated and given as inputs to the decoder.

4.5 Summary

One of the channel coding options provided in IEEE 802.16-2004 standard is the convolutional turbo coding. It outperforms the other channel coding options such as concatenated FEC and also is less complex than block turbo coding. The CTC encoder, interleaver and puncturer are described in detail and the procedure involved to calculate the CTC decoder input LLRs is described.

Chapter 5

Results and Conclusions

5.1 Performance of Concatenated STBC and CTC for WiMax

The Performance of a wireless system is significantly improved by the application of both multiple-input-multiple-output (MIMO) techniques and convolutional turbo codes (CTC). As we have seen in the previous chapters, MIMO techniques provide spatial diversity gain by combating the fading effects of the multipath channel and turbo codes provide significant coding gain. However, just using the space time block code (STBC), a type of MIMO technique without an outer channel code is not enough. Even soft decoding of STBC will not significantly improve the performance due to the lack of new extrinsic information [36]. Also, in slow fading channels, just turbo coding together with interleaving without MIMO cannot be that effective as delay and latency considerations limit the depth of interleaving. Deep fades can cause severe error propagation in the iterative decoding process [37]. Consequently it is desirable to concatenate the STBC with the CTC to simultaneously achieve the large diversity gains provided by the STBC and error correction capability of the CTC.

5.1.1 System Model for BWA Applications

The Rayleigh fading channel for broadband wireless access (BWA) systems exhibits slow fading as well as flat fading with no significant line-of-sight (LOS) component. Therefore,

channel response is constant over the entire length of a turbo codeword, and varies independently from frame to frame. A single-carrier system is considered for the simulations. Additive white Gaussian noise (AWGN) is added at the receiver for every received symbol. The randomly generated binary data couples of a particular frame size F are first turbo encoded by passing it through the CTC which constitutes of a double binary circular recursive systematic convolutional code (CRSC) with rate $1/3$. Alternate higher code rates are possible by puncturing the output obtained for rate $1/3$ as explained in Chapter 4. In our results we show and compare the bit-error-rate curves for code rates $1/3$, $1/2$, $3/4$. These turbo encoded bits which constitute the parity bits as well as the systematic bits are modulated by the QPSK ($M = 4$) symbol mapper as studied in Chapter 2. This mapper maps groups of two bits into one of four complex symbols from a unit power Gray coded QPSK constellation. Next, these QPSK symbols are transmitted by using two antennas ($n_T = 2$). We make use of the Alamouti space time block code (2Tx:1Rx) with two transmitters and one receiver to introduce transmit diversity as studied in Chapter 3. After space time coding, if OFDM were to be used, the resulting channel symbols would be transmitted through several sub-carriers which provides frequency diversity. However, we use a single carrier in our simulation to transmit the modulated symbols over the multipath fading wireless channel.

The signal gets distorted by the slowly fading channel as well as AWGN. The channel coefficients generated randomly for every turbo codeword, are uncorrelated circularly symmetric complex Gaussian with mean zero and unity variance. The noise random variables generated for every symbol, are uncorrelated circularly symmetric complex Gaussian with mean zero and variance σ^2 which varies with the average signal-to-noise-ratio (SNR). At the receiver, we assume the channel state information to be known and perform maximal ratio receiver combining (MRRC) to obtain the decision statistic vector \mathbf{d} as described in the STBC section in Chapter 3. At each time instance, the \mathbf{d} vector will have dimensions 2×1 , i.e. two symbols for the considered Alamouti STBC (2:1). These symbols have to be further processed in order to obtain the soft bits or the log likelihood ratios (LLRs) which are exploited by the turbo decoder. Calculation of these LLRs for STBC (2:1) with QPSK modulation is described in the last section of Chapter 4. For orthogonal STBCs, such as the Alamouti code, the complexity for computing these LLRs increases only linearly with the

number of transmit antennas. On the contrary, due to the lack of orthogonality, the complexity in calculating the LLRs rises exponentially with the number of transmit antennas when V-BLAST is used [38]. Finally, these soft bits are given as inputs to the CTC decoder to obtain the turbo decoded outputs. The turbo decoder uses the max-log-MAP algorithm [35].

5.2 Results

The performance results of the considered IEEE 802.16-2004 standard are shown in Fig. 5.1. These curves are obtained for frame size, $F = 24$ bytes and 16 iterations. We can see that there is a performance increase as the code rate decreases. In Fig. 5.3, the uncoded and coded STBC with $n_T = 2, n_R = 1$ for code rate $1/3$ are compared. We can see that there is a 4 dB difference between the curves which is attributed to the coding gain provided by the CTC. These curves are also compared with a single-input-single-output (SISO) turbo coded system in Fig. 5.4, where we can see that there is a diversity gain between the turbo coded SISO and STBC. In Fig. 5.2 throughput curves of the IEEE 802.16-2004 system for different code rates are shown. The throughput T is calculated by the equation $T = R(1 - FER)$, R being the code rate and FER being the frame error rate.

5.3 Conclusions

Fixed broadband wireless access is an ideal solution for providing high data rate communications where conventional systems like DSL and cable modems are either unavailable or too costly. It can be concluded that the performance of BWA systems can significantly be improved by space time block codes by providing diversity gain. Further improvement is achieved by concatenating the STBC with an outer channel code like a turbo code.

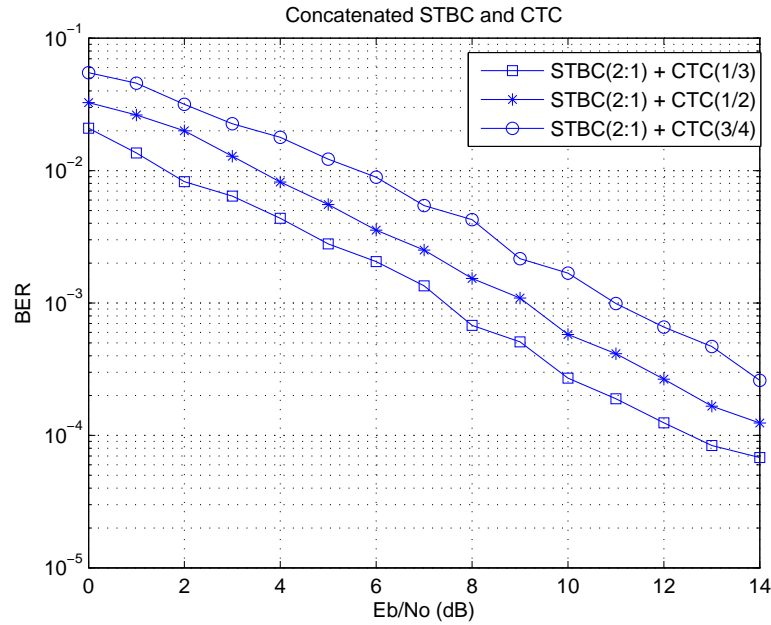


Figure 5.1: Concatenated STBC and CTC BER curves for code rates 1/3, 1/2, and 3/4.

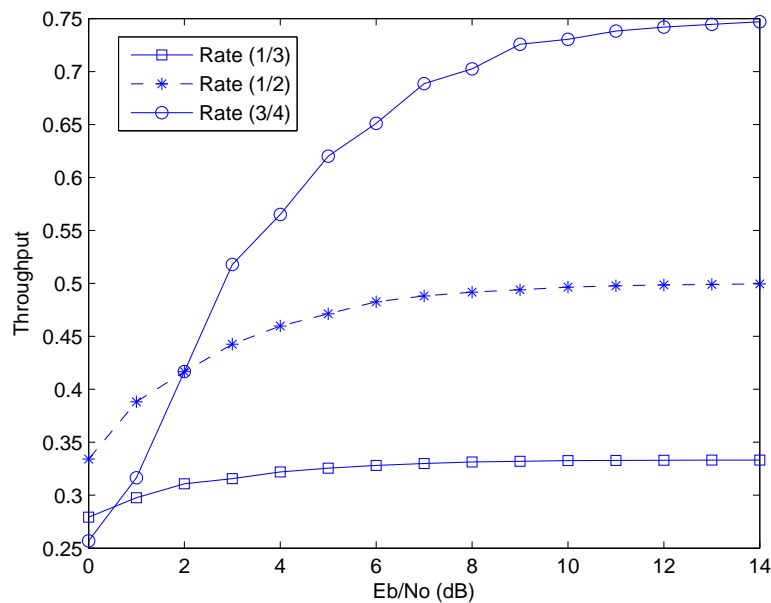


Figure 5.2: Throughput curves for concatenated STBC and CTC for rates 1/3, 1/2 and 3/4

5.4 Future Work

In this report, we considered only one of the MIMO techniques which is STBC to improve the performance of BWA systems. Though the STBC is very simple and improves the

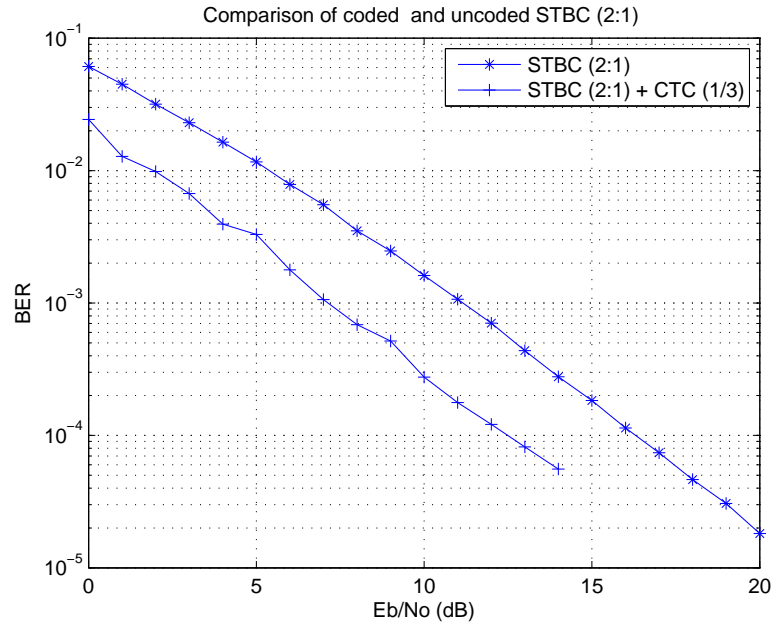


Figure 5.3: Comparison of coded and uncoded STBC for rate 1/3

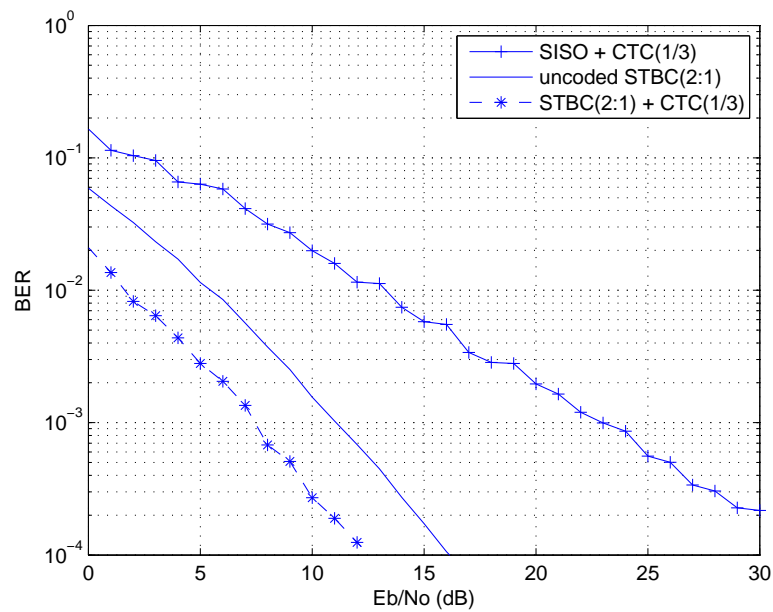


Figure 5.4: Comparison of SISO-CTC, uncoded STBC and coded STBC

reliability of the system, the data rates achieved are not as high as with V-BLAST. Also, we considered only a single carrier system because of which there is no frequency diversity. By

using OFDM, frequency diversity is exploited. Therefore a STBC-CTC or a V-BLAST-CTC with OFDM will give better performance. The concatenation of STBC with a block turbo code (BTC) might also be simple and lead to a performance improvement. Furthermore, since the row (or column) encoding (or decoding) of the BTC coding can be implemented in parallel, the computation efficiency can be further improved.

References

- [1] J. E. Gaskin, *Broadband Bible*, Wiley, 2004.
- [2] A. A. Gilroy and L. G. Kruger, “Broadband internet access: Background and issues,” CRS Issue Brief for Congress, Dec. 2003.
- [3] D.J. Johnston and M. LaBrecque, “IEEE 802.16 wirelessman specification accelerates wireless broadband access,” *Technology@Intel Magazine*, Aug. 2003.
- [4] H. Blcskei, A. J. Paulraj, K. V. S. Hari, and R. U. Nabar, “Fixed broadband wireless access: State of the art, challenges, and future directions,” *IEEE Commun. Magazine*, vol. 39, pp. 100–108, January 2001.
- [5] IEEE Computer Society, and IEEE Microwave Theory and Techniques, *IEEE 802.16-2004 standard for Local and metropolitan area networks. Part 16 : Air Interface for Fixed Broadband Wireless Access Systems*, October 2004.
- [6] A. Zakhia, Y. Peng, and Chang, J.M, “WiMax: The emergence of wireless broadband,” *IT Professional*, vol. 8, pp. 44–48, Jul-Aug 2006.
- [7] S. Nadkarni K. Seshadrinathan R. Simha l. J. Doyle, K. Han and I. C. Wong, “Performance evaluation of the IEEE 802.16a physical layer using simulation,” EE381K-11(14980)Wireless communication project report.
- [8] S. Alamouti, “A simple transmit diversity technique for wireless communications,” *IEEE J. Select. Areas Commun.*, vol. 16, no. 8, pp. 1451–1458, Oct. 1998.
- [9] G. Foschini, and M. Gans, “On the limits of wireless communications in a fading environment when using multiple antennas,” *Wireless Personal Commun.*, vol. 6, no. 3, pp. 311–335, 1998.
- [10] D. Reynolds, “Wireless communication systems,” Course Notes, WVU, Fall 2003.
- [11] A. Goldsmith, *Wireless Communication*, Cambridge University Press, 1995.
- [12] G. S. Prabhu and P. Mohana Shankar, “Simulation of flat fading using matlab for classroom instruction,” Department of Electrical and Computer Engineering, Drexel University.

- [13] R. Knopp, and P. A. Humblet, "On coding for block fading channels," *IEEE Trans. Inform. Theory*, vol. 46, pp. 189–205, January 2000.
- [14] T. Rappaport, *Wireless Communication Systems*, 3rd ed., New York, NY: McGraw-Hill, 1995.
- [15] B. Woerner, "Multi antenna systems," Course Notes, WVU, Spring 2005.
- [16] J.G. Proakis, *Digital Communications*, 3rd ed., New York, NY: McGraw-Hill, 1995.
- [17] N. Kong, "Performance of generalized selection diversity combining for both iid and noniid Rayleigh fading channels," *Proc. IEEE Military Commun. Conf. (MILCOM)*, pp. 1584–1589, 2004.
- [18] R. G. Gallager, *Information Theory and Reliable Communication*, Wiley, New York, NY, 1968.
- [19] V. Tarokh, N. Seshadri, and A. R. Calderbank, "Space-time codes for high data rate wireless communications: Performance criterion and code construction," *IEEE Trans. Inform. Theory*, vol. 44, no. 2, pp. 744–765, Mar. 1998.
- [20] G. Foschini, "Layered space-time architecture for wireless communication in a fading environment when using multi-element antennas," *Bell Labs. Tech. Journal*, vol. 1, no. 2, pp. 41–59, Autumn 1996.
- [21] L. Zheng, and D. Tse, "Diversity and multiplexing: A fundamental tradeoff in multiple antenna channels," *IEEE Trans. Inform. Theory*, vol. 49, pp. 1073–1096, May 2003.
- [22] V. Tarokh, H. Jafarkhani, and A. R. Calderbank, "Space-time block codes from orthogonal designs," *IEEE Trans. Inform. Theory*, vol. 45, no. 5, pp. 1456–1467, July 1999.
- [23] H. Jafarkhani, *Space-Time Coding*, Cambridge University Press, 2005.
- [24] I. S. Reed, and G. Solomon, "Polynomial codes over certain finite fields," *Journal of Applied Mathematics (SIAM)*, vol. 8, pp. 300–304, 1960.
- [25] P. Elias, "Coding for noisy channels," *IRE Conv. Rec.*, vol. 3, pp. 37–46, March 1955.
- [26] A. Ghosh, D. R. Wolter, J. G. Andrews, and R. Chen, "Broadband wireless access with WiMax/IEEE 802.16: Current performance benchmarks and future potential," *IEEE Commun. Magazine*, vol. 35, no. 9, 2005.
- [27] C. E. Shannon, "A mathematical theory of communication," *Bell Labs. Tech. Journal*, pp. 379–423 (Part 1); 623–56 (Part 2), July 1948.
- [28] S. Lin, and D. J. Costello, *Error Control Coding*, Prentice Hall, 2004.
- [29] B. Vucetic, and J. Yuan, *Turbo Codes*, Kluwer Academic Publishers, 2000.

- [30] C. Berrou, A. Glavieux, and P. Thitimajshima, “Near Shannon limit error-correcting coding and decoding,” *Proc. IEEE Int. Conf. on Commun. (ICC), Geneva, Switzerland*, vol. 2, pp. 1064 – 1070, May. 1993.
- [31] C. Berrou, C. Douillard, and M. Jezequel, “Multiple parallel concatenation of circular recursive convolutional (CRSC) codes,” *Annals of Telecommunication*, pp. 166–172, Mar.-Apr. 1999.
- [32] G. Richter B. Baumgartner, M. Reinhardt and M. Bossert, “Performance of forward error correction for IEEE 802.16e,” University of Ulm, and Siemens AG, October 2006.
- [33] M.C. Valenti, S. Cheng, and R. Iyer Seshadri, “Turbo and LDPC codes for digital video broadcasting” *Chapter 12 of Turbo code applications: A journey from a paper to realization*, Springer, 2005.
- [34] C. Berrou, R. Pyndiah, P. Adde, C. Douillard, and R. Le Bidan, “An overview of turbo codes and their applications,” *Wireless Technology. The European Conference on*, pp. 1–9, October 2005.
- [35] P. Robertson, P. Hoeher, and E. Villebrun, “Optimal and sub-optimal maximum a posteriori algorithms suitable for turbo decoding,” *European Trans. on Telecommun.*, vol. 44, no. 2, pp. 8(2):119–125, Mar./Apr. 1997.
- [36] G. Bauch, “Concatenation of space-time block codes and turbo-TCM,” *Proc. IEEE Int. Conf. on Commun. (ICC), Geneva, Switzerland*, vol. 2, pp. 1202–1206, June 1999.
- [37] H. El Gamal and A. R. Hammons, Jr., “Analyzing the turbo decoder using the Gaussian approximation,” *IEEE Trans. Inform. Theory*, vol. 47, pp. 671–686, Feb. 2001.
- [38] I. J. Wassell I. A. Chatzigeorgiou, M. R. D. Rodrigues and R. A. Carrasco, “Turbo coded OFDM / SC-FDE techniques for MIMO BFWA channels,” Technical report, Laboratory for Communication Engineering, University of Cambridge; Network Communications and Mobile Computing Research Group, University of Wolverhampton, Jan. 2005.